Journal of Engineering and Applied Research (JEAR)

National University of Skill

Winter & Spring 2026, Vol. 3, No. 1, p. 160-180

Journal Homepage: https://jear.tvu.ac.ir

:10.48301/jear.2025.527844.1126

Nonlinear vibration analysis of single-walled carbon nanotubes on radial-tangential mode using numerical methods

Zahra Azimzadeh [1*], Mohammad Reza Ebrahimian [2], Alireza Fatahi-Vajari [3]

[1] Department of Mathematics, YI.C., Islamic Azad University, Tehran, Iran.

[2] Department of Mechanical Engineering, Kar Higher Education Institute, Qazvin, Iran.

[3] Department of Mechanical Engineering, Shahr.C., Islamic Azad University, Shahryar, Iran.

ARTICLE INFO

Article Type:
Original Research

Received: 2025.06.10
Revised: 2025.09.10
Accepted: 2025.11.04

Keyword:
nonlinear coupled radial-tangential vibration
homotopy perturbation method
nonlocal theory
natural frequency
single-walled carbon nanotubes

***Corresponding Author:**
Zahra Azimzadeh
Email: *z.azimzadeh@iau.ac.ir*

ABSTRACT

This paper explores the nonlinear characteristics of coupled radial-tangential vibrations in single-walled carbon nanotubes (SWCNTs) using numerical methods. The authors derive two coupled partial differential equations governing these vibrations through the application of doublet mechanics (DM). The tangential vibration mode has been less studied in scientific researches due to the complexity of the governing equation. To calculate the nonlinear natural frequencies, they utilize the Homotopy Perturbation Method (HPM) to solve the derived equations. The analysis reveals that the coupling between the two vibration modes leads to complex natural frequency behaviors. The study examines how different boundary conditions, maximum vibration velocity, vibration modes, and geometrical parameters affect the nonlinear dynamics of these vibrations. In contrast to linear models, the nonlinear natural frequencies are influenced by the maximum vibration velocity; specifically, an increase in this velocity results in higher natural frequencies. However, as the tube diameter increases, the influence of the maximum vibration velocity decreases. Additionally, the study shows that the variations in nonlinear natural frequencies become more pronounced in higher vibration modes. To demonstrate the effectiveness of their method, the authors compare their findings with results from the fourth-order Runge-Kutta method, observing a strong correlation between both sets of results. The outcomes presented in this paper are original and offer a valuable benchmark for future investigations in this field.

E-ISSN: 3060-6357

Introduction

The analysis of mechanical behavior in heterogeneous solids typically diverges into two primary approaches, contingent on whether the constituent material phases exhibit a continuous or discrete distribution. In scenarios with continuous phase distribution, theoretical models often rely on continuum mechanics. However, these models generally do not incorporate scaling effects, which is often seen as a restriction when attempting to predict micromechanical material behavior [1, 2]. Due to the nanoscale size of carbon nanotubes (CNTs), conducting controlled experiments to determine the properties of a single CNT presents significant challenges [3–5]. Moreover, the implementation of molecular dynamics and atomistic simulation techniques [6–8] can be computationally expensive and time-intensive, especially for large-scale systems. To mitigate this limitation, several sophisticated adaptations to continuum mechanics have been introduced. These adaptations aim to integrate scaling and microstructural characteristics into the theoretical framework. These extended theories are generally classified as higher-order gradient continuum theories. Among these, doublet mechanics (DM) theory is a widely recognized approach in micromechanics. First developed by Granik and Ferrari [9], DM theory posits that the stress tensor at any given point is dependent on the strains present at all locations within the continuous material.

Since their discovery by Iijima in 1991 [10], carbon nanotubes (CNTs) have been recognized for their distinctive characteristics. The rapid advancement of nanotechnology has positioned nanotubes as promising candidates for diverse applications within nano-electronic-mechanical systems (NEMS). Consequently, there has been an increasing interest in these nanostructures. During operation, these components are frequently exposed to external loads, making the comprehension of their dynamic behavior, including resonant properties, crucial. Therefore, research focused on the free vibration characteristics of nanotubes under specific support conditions is vital, as these components can be integral to the design of nanosensors and nanoactuators. At the nanoscale, the mechanical properties of nanostructures often deviate significantly from those observed at the macroscopic level. This discrepancy is attributed to inherent size effects, which play a critical role in determining the performance of nanoscale materials and structures, impacting their mechanical, electronic, optical, and other properties. Mahdavinia et al. investigated the electrochemical properties of nanocomposite nanowires consisting of polyaniline and silver nanoparticles synthesized by the hard template method [11]. The challenge of measuring the properties of individual CNTs stems from their nanoscale dimensions [12].

Mirzamohammadi compared nickel-alumina nanocomposite coatings. The content of alumina nanoparticles has the greatest impact on these coatings. Also, the electrolyte composition was modified by adding Sodium dodecyl sulfate (SDS) [13]. Furthermore, the application of atomistic methods [7, 8] is often impractical for large-scale systems due to high computational costs and

lengthy processing times. Movahedi et al. discussed the effects of nanoparticles on oxidative stress and also its effect on improving the negative impact of other stresses [14]. The study of single-walled carbon nanotubes (SWCNTs) under dynamic loading is crucial due to their sensitivity to vibrations, which can lead to structural failure and affect system performance [15, 16]. Understanding the behavior of SWCNTs requires models that accurately reflect their dynamic characteristics, particularly considering the significant forms of vibrations: radial and tangential. Radial vibrations are particularly important when the CNT is stretchable, while tangential vibrations dominate in flexible CNTs that are subjected to external forces. The coupling between these two types of vibrations can complicate the analysis, as factors like cracks or unbalance can exacerbate the interaction between radial and tangential motions.

Most existing research has tended to focus on individual vibrational modes—flexural [17- 20], torsional [21- 24], radial [25, 26], or longitudinal [27-29]—without adequately addressing the coupling effects. This oversight can lead to inaccurate predictions of the dynamic behavior of SWCNT systems, which is critical for ensuring their safe operation. The complexity of coupled vibrations, especially in terms of radial-tangential interactions, arises from the nonlinearity introduced by large deformations. When these couplings are not considered, the accuracy of calculations may suffer, and essential characteristics of the CNTs could be overlooked. An accurate model that incorporates these coupled vibrations is therefore essential for predicting the performance and longevity of CNT-based systems, particularly in applications demanding high reliability. In summary, investigating the coupled radial-tangential vibrations of SWCNTs is vital for enhancing the understanding of their dynamic behavior and ensuring the integrity of systems that utilize these materials. However, most of the investigations conducted on the radial and tangential vibration of CNTs have been restricted to the linear theory. The HPM as a powerful analytical approach was first introduced by He [30, 31] for solving various linear and nonlinear initial and boundary value problems. The HPM in applied mathematics is widely studied now by most mathematicians. In this method, the solution is considered as the sum of an infinite series which converges rapidly to the exact solution. Usually, one or two iterations lead to high accuracy of the solution. The series used is a series of functions rather than terms as is in Taylor series. The method has recently been applied to a wide class of differential and integral equations, stochastic and deterministic problems, linear and non-linear equations. The advantages of this method to other methods is more simplicity, give better results and with time saving because in this method convergence is especially rapid in the non-linear and nonhomogeneous equations. The HPM was also studied by many mathematicians and engineers to investigate nonlinear equations arising in science and engineering. This simple method has been applied to solve linear and nonlinear equations in different fields of mechanics like heat transfer, fluid mechanics and so on [32- 34]. Ebrahimian et al. studied bending behavior of Euler-Bernoulli and Timoshenko nanobeams using DM By taking the effect of the scale parameter explicitly and chiral effect into account [19]. In another work, the torsion of nanotubes embedded in an elastic medium is studied using

doublet mechanics wherein the governing equations take the effects of scale parameter and chirality explicitly and simultaneously into account [35]. Shokri et al. presented a detailed analytical investigation into the nonlinear buckling behavior of a composite rectangular plate reinforced with graphene nanosheets (GNSs) using the third-order shear deformation theory (TSDT) [4]. A new approach is applied using doublet mechanics (DM) by Ebrahimian where the governing equation are obtained using shell equilibrium equations and solved by angular displacement expansions with considering the scale parameter [24].

This study investigates the coupled nonlinear radial-tangential vibrations of single-walled carbon nanotubes (SWCNTs), a topic of significant interest due to its implications in nanotechnology and materials science. The integration of geometric nonlinearity with vibrational coupling effects provides a comprehensive framework for elucidating the dynamic responses of SWCNTs. Employing nonlocal elasticity theory; the governing differential equations are derived to capture the complex behavior inherent in these nanostructures. The resulting system comprises two coupled partial differential equations describing the interactions between radial and tangential displacements. To solve these equations and determine the natural frequencies, the Homotopy Perturbation Method (HPM) is utilized, leveraging its proven effectiveness in addressing nonlinear problems with rapid convergence characteristics. The present work quantitatively identifies principal factors influencing the coupled vibrational behavior; thereby enhancing the understanding of the mechanical properties of SWCNTs. Validation of the fundamental frequencies against experimental data and results from continuum modeling confirms the robustness of the proposed theoretical approach. Furthermore, the successful application of HPM underscores its potential as a reliable analytical method for nonlinear dynamic analysis. A comparative assessment between HPM and numerical solutions for amplitude-frequency responses further demonstrates the accuracy and practicality of the method.

The structure of the paper is as follows. In Sect.2, a brief review to derive the nonlinear equation of motion for coupled radial-tangential vibration of SWCNTs is given using nonlocal theory. In Sect.3, the equation of motion for SWCNTs in tangential-radial vibration is solved using HPM and the natural frequencies are obtained. In Sect.4, the obtained nonlinear natural frequencies are compared with numerical results to illustrate the ability and accuracy of the proposed method. In Sects.5 a brief discussion and conclusions follows.

Derivation of nonlinear equation of motion for coupled radial-tangential vibration of SWCNTs

In this section, we establish the coupled tangential-radial governing differential equations that describe the vibrational characteristics of single-walled carbon nanotubes (SWCNTs). We utilize shell theory, while disregarding the influence of rotary inertia and gyroscopic moments. Considering both radial and tangential deformations, we assume significant vibration amplitude. This leads to the inclusion of stretching nonlinearity, which stems from the

extension of the shaft centerline. The orthogonal coordinate system axes (r, θ, z) align with the normal, tangent, and axial axes in cylindrical coordinates. The displacements of a sample element's center along the normal, tangent, and axial axes are represented by u_r, u_θ and u_z, respectively. Additionally, θ denotes the torsional deformation of the cross-section around the z-direction. The fundamental equations of motion for cylindrical coordinates are based on reference [21].

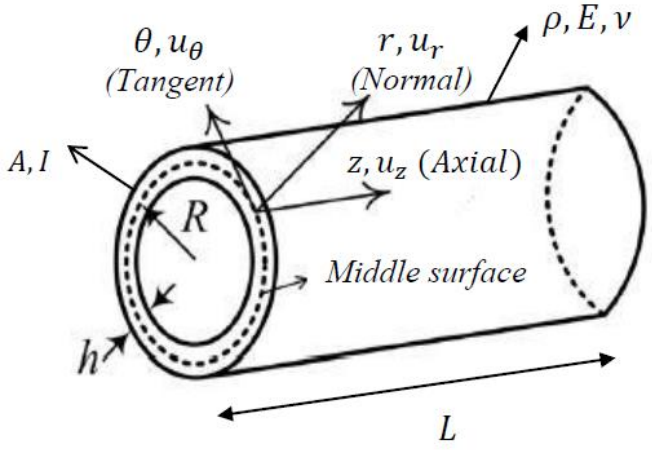

Figure 1. A nanotube in cylindrical coordinate [21]

The equations of motion in cylindrical coordinates are expressed as follows [25]:

$$\frac{\partial N_{zr}}{\partial z}+\frac{1}{r}\frac{\partial N_{\theta r}}{\partial \theta}-\frac{N_{\theta\theta}}{r}+\rho f_r=\rho\frac{\partial^2 u_r}{\partial t^2} \quad (1)$$

$$\frac{\partial N_{z\theta}}{\partial z}+\frac{1}{r}\frac{\partial N_{\theta\theta}}{\partial \theta}+\frac{N_{\theta r}}{r}+\rho f_\theta=\rho\frac{\partial^2 u_\theta}{\partial t^2} \quad (2)$$

$$\frac{\partial N_{zz}}{\partial z}+\frac{1}{r}\frac{\partial N_{\theta z}}{\partial \theta}+\rho f_z=\rho\frac{\partial^2 u_z}{\partial t^2} \quad (3)$$

$$\frac{\partial M_{zz}}{\partial z}+\frac{1}{r}\frac{\partial M_{\theta z}}{\partial \theta}+\rho\bar{l}_z=N_{zr} \quad (4)$$

$$\frac{\partial M_{z\theta}}{\partial z}+\frac{1}{r}\frac{\partial M_{\theta\theta}}{\partial \theta}+\frac{1}{r}M_{\theta r}+\rho\bar{l}_\theta=N_{\theta r} \quad (5)$$

$$\frac{M_{zr}}{\partial z}+\frac{1}{r}\frac{M_{\theta r}}{\partial \theta}-\frac{M_{\theta\theta}}{r}+\rho\bar{l}_r=N_{rr} \quad (6)$$

where f_i and $\bar{l}_i$ represent body forces and body moments, respectively. Equations (1) through (6) constitute the motion equations for a thin shell in cylindrical coordinates and require solving to facilitate the dynamic analysis of the system. N_{ij} and M_{ij} signify resultant forces and moments, respectively, and are defined by the subsequent equations [21]:

$$N_{ij}=\int_{-\frac{h}{2}}^{\frac{h}{2}}\sigma_{ij}^{(M)}dz \ , i,j=1,2,3 \quad (7)$$

$$M_{ij}=\int_{-\frac{h}{2}}^{\frac{h}{2}}z\sigma_{ij}^{(M)}dz \ , i,j=1,2,3 \quad (8)$$

This study adopts the subsequent assumptions, referred to as Love's first approximation, for cylindrical shells [24]:

1. Points lying on a normal to the middle surface before deformation remain on the normal after deformation. Consequently, the transverse shear stresses $\sigma_{rz}^{(M)}$ and $\sigma_{\theta r}^{(M)}$ are considered negligible.

2. Displacements are small relative to the shell thickness.

3. Normal stresses in the thickness direction ($\sigma_{rr}^{(M)}$) are negligible, assuming a planar state of stress.

Assuming axisymmetry and homogeneity throughout the nanotube, and considering that the nanotube vibrates solely in radial and tangential modes—where the tube's cross-section remains undeformed elastically—and further neglecting body forces, it can be inferred that:

$$\frac{\partial}{\partial z} = \frac{\partial}{\partial r} = 0, u_z = 0 \quad (9)$$

Under such assumptions, Eqs. (1)- (6) are reduced to

$$-\frac{N_{\theta\theta}}{r} = \rho \frac{\partial^2 u_r}{\partial t^2} \quad (10)$$

$$\frac{1}{r}\frac{\partial N_{\theta\theta}}{\partial \theta} = \rho \frac{\partial^2 u_\theta}{\partial t^2} \quad (11)$$

These resulting equations represent the equations of motion governing the coupled tangential-radial vibration of single-walled carbon nanotubes (SWCNTs).

To incorporate the scale effect into these equations of motion, we employ the concept of a Doublet Mechanics (DM). Figure 2 illustrates a doublet, which serves as a fundamental constitutive unit within DM. For any given doublet (A, B), there exists a corresponding doublet or branch vector $\boldsymbol{\zeta}_a$, connecting the centers of adjacent particles and defining the doublet axis. The magnitude of this vector, denoted as $\eta_a = |\boldsymbol{\zeta}_a|$, is referred to as the length scale. In the case of particles in direct contact, the length scale simply represents the particle diameter. However, particles need not always be in contact; therefore, the length scale η_a can be used more generally to represent a broader range of microstructural features.

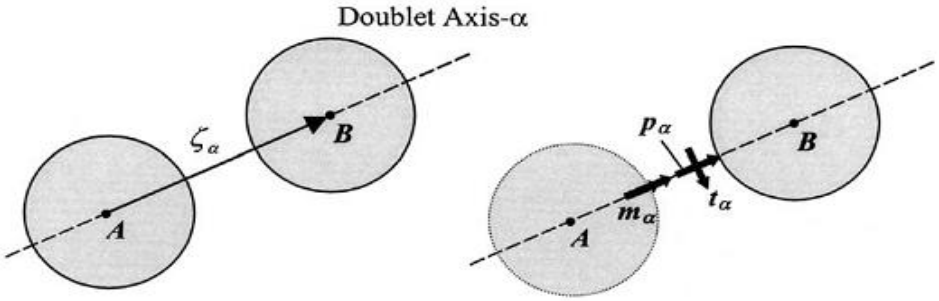

Figure 2. Doublet [27**]**

As previously mentioned, the kinematic framework allows for relative elongational, shearing, and torsional movements between particles. This is leveraged to define an elongational microstress p_a, a shear microstress t_a, and a torsional microstress m_a, as depicted in Figure 2. It is important to note that these microstresses are not second-order tensors in the conventional continuum mechanics sense. Instead, they are vector quantities that represent the elastic microforces and microcouples governing the interaction between doublet particles. Examples include the interatomic forces between carbon molecules within a nanotube. The orientation of these microstresses is dictated by the doublet axes, which are determined by the material's microstructure. These microstresses are not continuously distributed but are rather localized to specific points within the medium being modeled using DM.

In contrast to the linear algebraic relationships between stress and strain in local theories, the nonlocal DM theory yields differential relationships involving both stress and strain. The following presents these relationships for homogeneous nanotubes, assuming that nonlocal behavior is insignificant in the thickness direction. The nonlocal DM constitutive relation for macroscopic stress is then specifically defined for nanotubes as follows [25, 27]:

$$\sigma_{\theta\theta} = \frac{E}{r^2(1-\nu^2)}\left(\varepsilon_{\theta\theta} + \kappa\eta^2 \frac{\partial^2 \varepsilon_{\theta\theta}}{\partial z^2}\right) \tag{12}$$

where E represents Young's modulus of the nanotubes, and κ is a coefficient that depends on the chirality of the tube. It is evident that when the nonlocal parameter η is zero, the constitutive relations of local theories are recovered. Substituting Equations (12) into Equation (7) yields the nonlocal stress resultants as:

$$N_{\theta\theta} = \frac{Eh}{r^2(1-\nu^2)}\left(\varepsilon_{\theta\theta} + \kappa\eta^2 \frac{\partial^2 \varepsilon_{\theta\theta}}{\partial z^2}\right) \tag{13}$$

It is important to note that the macromodulus in constitutive Equation (13), corresponding to the first approximation ($\eta = 0$), is non-scale-dependent and, in fact, independent of chirality, implying isotropy within the plane (independence from scale). Conversely, the macromoduli in higher approximations exhibit anisotropy. This leads to the conclusion that, in the first approximation, Equation (13) models the continuum-like behavior of solids,

while in subsequent approximations, Equation (13) also reflects the discrete-like characteristics of the solid [17]. Therefore, it can be concluded that DM theory possesses the capability to model solids, considering their dual and, to some extent, contradictory discrete-continuous nature. The strength of this dual-representation capability is evident in the discussion of isotropy. The basal plane of the SWCNT exhibits isotropy only in the continuum (non-scale) approximation. Thus, isotropy becomes a scale-related concept. In reality, no material can be definitively argued to be isotropic across all dimensional scales, extending down to its most elementary component level [1]. The nonlinear strain-displacement relation is written as [2]:

$$\boldsymbol{\varepsilon} = \frac{1}{2}(\boldsymbol{\nabla u} + \boldsymbol{\nabla u}^T + \boldsymbol{\nabla u}^T \boldsymbol{\nabla u}) \tag{14}$$

where $\boldsymbol{\nabla}$ is the gradient operator in cylindrical coordinates given as [25]

$$\boldsymbol{\nabla} = \frac{\partial}{\partial r}\boldsymbol{e}_r + \frac{1}{r}\frac{\partial}{\partial \theta}\boldsymbol{e}_\theta + \frac{\partial}{\partial z}\boldsymbol{e}_z \tag{15}$$

In cylindrical coordinate, $\boldsymbol{\nabla u}$ can be written as [21]

$$\boldsymbol{\nabla u} = \begin{bmatrix} \frac{\partial u_r}{\partial r} & \frac{1}{r}\left(\frac{\partial u_r}{\partial \theta} - u_\theta\right) & \frac{\partial u_r}{\partial z} \\ \frac{\partial u_\theta}{\partial r} & \frac{1}{r}\left(\frac{\partial u_\theta}{\partial \theta} + u_r\right) & \frac{\partial u_\theta}{\partial z} \\ \frac{\partial u_z}{\partial r} & \frac{1}{r}\frac{\partial u_z}{\partial \theta} & \frac{\partial u_z}{\partial z} \end{bmatrix} \tag{16}$$

Substituting Eq. (16) into Eq. (14) and making some manipulations along with considering Eq. (9), yields

$$\varepsilon_{\theta\theta} = \frac{u_r}{r} + \frac{1}{2r^2}\left(\frac{\partial u_\theta}{\partial \theta} + u_r\right)^2 \tag{17}$$

Now, substituting Eq. (17) into Eq. (13) and the results into Eqs. (10) and (11) with making some manipulations with neglecting scale effect yields

$$-\frac{E}{r^2(1-\nu^2)}\left[u_r + \frac{1}{2r}u_r^2 + \frac{1}{2r}\left(\frac{\partial u_\theta}{\partial \theta}\right)^2 + \frac{1}{r}u_r\frac{\partial u_\theta}{\partial \theta}\right] = \rho\frac{\partial^2 u_r}{\partial t^2} \tag{18}$$

$$\frac{E}{r^2(1-\nu^2)}\left[\frac{1}{r}\frac{\partial u_r}{\partial \theta} + \frac{1}{r^2}u_r\frac{\partial u_\theta}{\partial \theta} + \frac{1}{r^2}\frac{\partial u_\theta}{\partial \theta}\frac{\partial^2 u_\theta}{\partial \theta^2} + \frac{1}{r^2}\frac{\partial u_r}{\partial \theta}\frac{\partial u_\theta}{\partial \theta} + \frac{1}{r^2}u_r\frac{\partial^2 u_\theta}{\partial \theta^2}\right] = \rho\frac{\partial^2 u_\theta}{\partial t^2} \tag{19}$$

Equations (20) and (21) represent the equations of motion for the nonlinear coupled vibration of SWCNTs. These equations demonstrate that, due to the presence of nonlinear terms, the two equations are interconnected. The fundamental linear equations can be easily derived by setting the nonlinear terms to zero, which results in decoupling the two equations.

Application of HPM for solving nonlinear vibrations of SWCNTs

This section focuses on solving the nonlinear governing equations for the coupled radial-tangential vibration of SWCNTs. The deflection of the nanotube is subject to the following boundary conditions in the radial and tangential directions, respectively.

For two clamped (C-C) boundary conditions [21]:

$$u_r(\theta,t)=0, u_\theta(\theta,t)=0, at\ \theta=0,\pi \tag{20}$$

For two free (F-F) boundary conditions [21]

$$\frac{\partial u_r(\theta,t)}{\partial\theta}=0, \frac{\partial u_\theta(\theta,t)}{\partial\theta}=0, at\ \theta=0,\pi \tag{21}$$

For clamped-free (C-F) boundary condition [21]

$$u_r(\theta,t)=0, u_\theta(\theta,t)=0\ at\ \theta=0, \frac{\partial u_r(\theta,t)}{\partial\theta}=0, \frac{\partial u_\theta(\theta,t)}{\partial\theta}=0\ at\ \theta=\pi \tag{22}$$

Table 1. Common boundary conditions for the tangential direction [27]

End conditions of beam	Mode shape (normal function)
Two boundaries clamped (C-C)	$sin(n\theta)$
Two boundaries free (F-F)	$cos(n\theta)$
Clamped-free (C-F)	$1-cos(2n\theta)$

Now, the nonlinear equations of motion are solved to obtain the nonlinear natural frequencies. We Assume $u_r(\theta,t)=\varphi(\theta)U(t)$ and $u_\theta(\theta,t)=\psi(\theta)W(t)$where $\varphi(\theta)$ and $\psi(\theta)$ are the eigenmodes of the tube satisfies the kinematic boundary conditions and $U(t)$ and $W(t)$ are the time-dependent deflection parameters of the nanotube. The base functions corresponding to the above boundary conditions are given in Table 1.

Now, we apply the Galerkin method to obtain the governing equations of motion as follows:

$$-\frac{E}{\rho r^2(1-\nu^2)}\left[a_1U+\frac{1}{2r}a_2U^2+\frac{1}{2r}a_3W^2+\frac{1}{r}a_4\mathrm{UW}\right]=a_1\frac{\partial^2U}{\partial t^2} \tag{23}$$

$$\frac{E}{\rho}\left[\frac{1}{r}a_5\mathrm{U}+\frac{1}{r^2}a_6\mathrm{UW}+\frac{1}{r^2}a_7\mathrm{W}^2+\frac{1}{r^2}a_8\mathrm{UW}+\frac{1}{r^2}a_9\mathrm{UW}\right]=a_{10}\frac{\partial^2W}{\partial t^2} \tag{24}$$

The following initial conditions apply to these differential equations, which model the nonlinear and coupled motion of single-walled carbon nanotubes (SWCNTs) in both tangential and radial directions [27].

$$U(0)=0, \frac{dU}{dt}(0)=U_{max} \tag{25}$$

$$W(0)=0, \frac{dW}{dt}(0)=W_{max} \tag{26}$$

wherein U_{max} and W_{max} denote the maximum velocities of oscillation in circumferential and radial directions, respectively. In Eqs. (23) and (24), $\alpha_1,\alpha_2,\ldots,\alpha_{10}$ are as follows:

$$\alpha_1=\int_0^L\varphi^2(\theta)d\theta\,,\alpha_2=\int_0^L\varphi^3(\theta)d\theta\,,\alpha_3=\int_0^L\psi'^2(\theta)\varphi(\theta)d\theta\,,\alpha_4=\int_0^L\psi'(\theta)\varphi^2(\theta)d\theta \tag{27}$$

$\alpha_5 = \int_0^L \varphi'(\theta)\psi(\theta)d\theta\,, \alpha_6 = \int_0^L \varphi(\theta)\psi'(\theta)\psi(\theta)d\theta\,, \alpha_7 = \int_0^L \psi''(\theta)\psi'(\theta)\psi(\theta)d\theta\,, \alpha_8 = \int_0^L \varphi'(\theta)\psi'(\theta)\psi(\theta)d\theta\,, \alpha_9 = \int_0^L \varphi(\theta)\psi''(\theta)\psi(\theta)d\theta\,, \alpha_{10} = \int_0^L \psi^2(\theta)d\theta$
(28)

Changing the variable $\tau = \omega t, \nu = \Omega t, a = \frac{U}{r}, b = \frac{W}{r}$ and $r = \sqrt{\frac{I}{A}}$, Eqs. (23) and (24) can be transformed to the following nonlinear equation:

$\omega^2 \frac{d^2a}{\partial\tau^2} + Aa + Ba^2 + Cb^2 + Dab = 0$ (29)

$\Omega^2 \frac{d^2b}{\partial\nu^2} + Ea + Fb^2 + Gab = 0$ (30)

wherein ω and Ω are the nonlinear radial and tangential frequencies in the coupled nonlinear tangential-radial vibration of SWCNTs. The coefficients A, B, C, D and E are defined by the following equations

$A = \frac{E}{\rho r^2(1-\nu^2)} = \omega_L^2$ (31)

$B = \frac{E}{2\rho r^3(1-\nu^2)} \frac{\alpha_2}{\alpha_1} \sqrt{\frac{I}{A}}$ (32)

$C = \frac{E}{2\rho r^3(1-\nu^2)} \frac{\alpha_3}{\alpha_1} \sqrt{\frac{I}{A}}$ (33)

$D = \frac{E}{\rho r^3(1-\nu^2)} \frac{\alpha_4}{\alpha_1} \sqrt{\frac{I}{A}}$ (34)

$E = -\frac{E}{\rho}\frac{\alpha_4}{\alpha_7} = \Omega_L^2$ (35)

$F = \left(-\frac{I}{A}\frac{\alpha_7}{\alpha_{10}}\right)\frac{E}{\rho}$ (36)

$G = \left(-\frac{I}{A}\frac{\alpha_6+\alpha_8+\alpha_9}{\alpha_{10}}\right)\frac{E}{\rho}$ (37)

In Eqs. (31) and (35), $\omega_L = \sqrt{A}$ and $\Omega_L = \sqrt{E}$ is the linear, free vibration frequency in the tangential and radial vibration modes, respectively and the unknown angular frequency has to be determined. To this end, New HPMs are applied to seek the solution of Eqs. (29) and (30). The following homotopies with ω_0 and Ω_0 as the initial approximations for the angular frequency are considered

$(1-p)\omega_0^2\left(\frac{d^2a}{\partial\tau^2} + Aa\right) + p\left(\omega^2\frac{d^2a}{\partial\tau^2} + Aa + Ba^2 + Cb^2 + Dab\right) = 0$ (38)

$(1-p)\Omega_0^2\left(\frac{d^2b}{\partial\nu^2} + Eb\right) + p\left(\Omega^2\frac{d^2b}{\partial\nu^2} + Ea + Fb^2 + Gab\right) = 0$ (39)

Here p is a parameter, $a = a(\tau, p)$, $b = b(\nu, p)$, $\omega = \omega(p)$ and $\Omega = \Omega(p)$. Obviously, when $p = 0$, Eqs. (38) and (39) yields the following linear harmonic equations

$\frac{d^2a}{\partial\tau^2} + Aa = 0, a(0) = 0, \frac{da(0)}{d\tau} = X$ (40)

$$\frac{d^2b}{\partial v^2} + Eb = 0, b(0) = 0, \frac{db(0)}{dv} = Y \tag{41}$$

It is notable that for $p = 1$, it results the nonlinear Eqs. (29) and (30), respectively. As embedding parameter p varied from 0 to 1, the solutions $a = a(\tau, p)$ and $\omega = \omega(p)$ along with $b = b(v, p)$ $\Omega = \Omega(p)$ of the homotopy Eqs. (38) and (39) change from their initial approximations $a_0(\tau), \omega_0$ and $b_0(v), \Omega_0$ to the required solutions $a(\tau), \omega$ and $b(v), \Omega$ of Eqs. (29) and (30), respectively. Suppose the solution of Eqs. (29) and (30) to be in the following forms [33]:

$$a(\tau) = a_0(\tau) + pa_1(\tau) + \cdots \tag{42}$$

$$\omega = \omega_0 + p\omega_1 + \cdots \tag{43}$$

$$b(v) = b_0(v) + pb_1(v) + \cdots \tag{44}$$

$$\Omega = \Omega_0 + p\Omega_1 + \cdots \tag{45}$$

Substituting the above relations into the Eqs. (38) and (39), respectively and equaling the coefficients of the terms with same powers of p, the following linear differential equations are obtained

$$\begin{aligned} &p^0: \frac{d^2a_0}{\partial \tau^2} + Aa_0 = 0\,, a_0(0) = 0\,, \frac{da_0(0)}{\partial \tau} = X \\ &p^1: \omega_0^2\left(\frac{d^2a_1}{\partial \tau^2} + Aa_1\right) + \left(\omega^2\frac{d^2a_0}{\partial \tau^2} + Aa_0 + Ba_0^2 + Cb_0^2 + Da_0b_0\right) = 0\,, a_1(0) = 0\,, \frac{da_1(0)}{\partial \tau} = 0 \\ &\vdots \end{aligned} \tag{46}$$

$$\begin{aligned} &p^0: \frac{d^2b_0}{\partial v^2} + Eb_0 = 0\,, b_0(0) = 0\,, \frac{db_0(0)}{\partial v} = Y \\ &p^1: \Omega_0^2\left(\frac{d^2b_1}{\partial v^2} + Eb_1\right) + \left(\Omega^2\frac{d^2b_0}{\partial v^2} + Ea_0 + Fb_0^2 + Ga_0b_0\right) = 0\,, b_1(0) = 0\,, \frac{db_1(0)}{\partial v} = 0 \\ &\vdots \end{aligned} \tag{47}$$

The solution of the initial zeroth approximation is simply given by

$$a_0(\tau) = Xsin(\tau) \tag{48}$$

$$b_0(v) = Ysin(v) \tag{49}$$

wherein X and Y can be known as maximum radial vibration velocity (MRVV) and maximum tangential vibration velocity (MTVV), respectively.

Substituting Eqs. (48) and (49) into the first approximations of Eqs. (46) and (47), respectively, it is obtained

$$\omega_0^2\left(\frac{d^2a_1}{\partial\tau^2}+Aa_1\right)+[-\omega_0^2Xsin(\tau)+AXsin(\tau)+BX^2sin^2(\tau)+CY^2sin^2(\nu)+DXYsin(\tau)sin(\nu)]=0 \quad (50)$$

$$\Omega_0^2\left(\frac{d^2b_1}{\partial\tau^2}+Eb_1\right)+[-\Omega_0^2Ysin(\nu)+EXsin(\tau)+FY^2sin^2(\nu)+GXYsin(\nu)sin(\tau)]=0 \quad (51)$$

Expanding the trigonometric function using Fourier sine series for $sin^2(\beta)$ in the first period yields

$$sin^2(\beta)\cong\frac{8}{3\pi}sin(\beta)-\frac{8}{15\pi}sin(3\beta) \quad (52)$$

Substituting Eq. (52) into Eqs. (50) and (51) and letting the coefficient of $sin(\tau)$ and $sin(\nu)$ to be zero in order to eliminate the secular terms, it is found that

$$\omega=\sqrt{A+\frac{8}{3\pi}\left(BX+C\frac{Y^2}{X}+DY\right)} \quad (53)$$

$$\Omega=\sqrt{E\frac{X}{Y}+\frac{8}{3\pi}(FY+GX)} \quad (54)$$

The analysis reveals that, unlike linear systems, the vibration frequencies are dependent on the velocity amplitude, which is inherently linked to the initial conditions. Consequently, as the amplitude increases, the divergence between the linear and nonlinear frequencies becomes more noticeable due to the system's nonlinearity. It's important to note that neglecting the frequency dependence on vibration amplitudes yields the linear natural frequencies of the system. The results indicate that the nonlinear tangential natural frequency deviates from its linear counterpart solely based on the tangential vibration amplitude. In contrast, the nonlinear radial natural frequency is contingent on both the tangential and radial vibration velocities of the system.

Considering Equations (53) and (54), the solution of Equations (50) and (51) can be obtained as:

$$a_1(\tau)=-\frac{1}{15\pi\omega_0^2}(BX^2+CY^2+DXY)sin(3\tau) \quad (55)$$

$$b_1(\nu)=-\frac{1}{15\pi}(FY^2+GXY)sin(3\nu) \quad (56)$$

Thus, the first approximate solution of Eqs. (29) and (30) can be written as follows:

$$a(\tau)=a_0(\tau)+a_1(\tau)=X\sin(\tau)-\frac{1}{15\pi\omega_0^2}\left(BX^2+CY^2+DXY\right)\sin(3\tau) \quad (57)$$

$$b(\nu)=b_0(\nu)+b_1(\nu)=Y\sin(\nu)-\frac{1}{15\pi\Omega_0^2}\left(FY^2+GXY\right)\sin(3\nu) \quad (58)$$

Results and Discussion

This section presents a comparison between the results obtained using the Homotopy Perturbation Method (HPM) and available numerical results to validate the presented method.

To demonstrate the accuracy of the obtained analytical results, the variation of the non-dimensional vibration amplitude for tangential modes is plotted versus the non-dimensional time for a Zigzag (16, 0) SWCNT using the fourth-order Runge-Kutta method and the HPM in Figure 3. This figure shows that the HPM predictions of the nonlinear tangential frequency are in good agreement with the fourth-order Runge-Kutta numerical results. The boundary condition is assumed to be clamped-free.

Experimentally, the natural frequency is related to the angular frequency ω via $f=\frac{\omega}{2\pi}$. This relation is used in Figures 4-7 to report the frequencies in THz. Throughout this paper, the material properties of the SWCNT are taken to be: Young's modulus $E=1.1\,TPa$, mass density $\rho=2300\ \frac{kg}{m^3}$, and Poisson's ratio $\nu=0.2$ [1]. In the Discrete-to-Continuum (DM) model, the scale parameter used is the carbon-carbon bond length $\eta=0.1421\,nm$ [17].

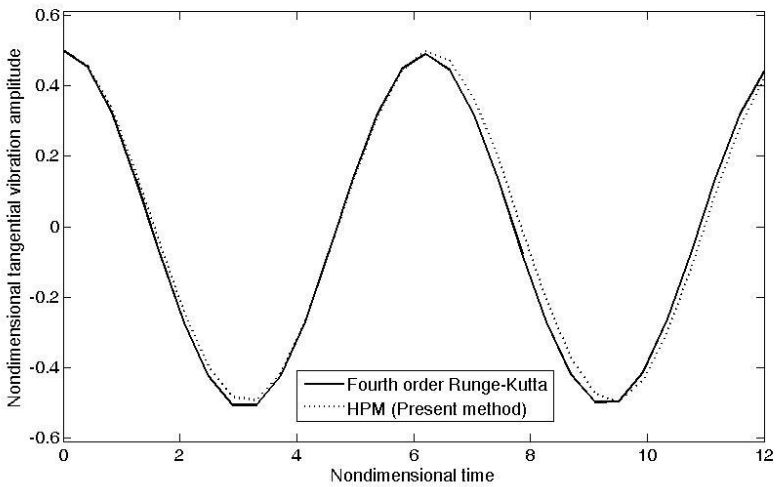

Figure 3. Nondimensional tangential vibration amplitude versus nondimensional time for Zigzag (16, 0) nanotube with $X=Y=1$ for clamped-free boundary condition

Another validation is done with comparing the radial vibration frequency with [36] in table 1. It is obvious that there is a good agreement between this method and the method presented in [36].

Table 1 shows the radial frequencies of different Zigzag and Armchair SWCNTs based on the available analytical and experimental results presented here. The first column shows the n and m chiral indices of the nanotube; the second and third columns show the SWCNT diameter (d, in nm) and length (L, nm), respectively. The next two columns are the analytical and experimental results.

From Table 1, it can be seen that the doublet mechanical predictions of the radial frequencies of different SWCNTs are in good agreement with the available experimental results. The difference between the results may be due to the interactions and coupling effect between tangential and radial vibration.

Table 1. Comparison between radial frequencies in coupled radial-tangential vibration with experimental radial vibration (cm^{-1}) for different SWCNTs.

Tube (n, m)	Diameter (nm)	Length (nm)	Radial frequency obtained using DM (present method)	radial frequency obtained in [36] using experimental result
(3,3)	0.4069	6.0	538.3	549.3
(6,0)	0.4698	7.0	471.2	475.7
(4,4)	0.5425	8.0	409.7	412.0
(7,0)	0.5481	9.0	406.9	407.8
(8,0)	0.6264	10.0	355.8	356.8
(5,5)	0.6781	10.5	328.1	329.6
(9,0)	0.7047	11.0	317.9	317.2
(10,0)	0.7830	12.0	286.3	285.4
(6,6)	0.8138	12.5	274.7	274.6
(11,0)	0.8613	13.0	260.6	259.5
(12,0)	0.9397	14.0	238.3	237.8
(7,7)	0.9494	14.5	236.1	235.4
(8,8)	1.0850	15.0	207.6	206.0
(13,0)	1.0180	15.5	220.5	219.5
(14,0)	1.0963	16.0	204.9	203.9
(15,0)	1.1746	17.0	190.9	190.3
(9,9)	1.2206	17.5	184.1	183.1
(16,0)	1.2529	18.0	179.1	178.4
(17,0)	1.3312	19.0	169.4	167.9
(10,10)	1.3563	19.5	165.3	164.8
(18,0)	1.4095	20.0	159.5	158.6
(19,0)	1.4878	21.0	151.3	150.2
(20,0)	1.5661	22.0	143.9	142.7

Figures 4 and 5 depict the relationship between nonlinear natural frequencies with respect to MRVV and MTVV for a Zigzag (16, 0) nanotube, respectively. These figures illustrate that, unlike linear systems, the nonlinear natural frequencies are dependent on the maximum vibration velocity. Specifically, as the velocity increases, the difference between the linear and nonlinear frequencies becomes more significant. It's important to note that when the terms $B = C = D = 0$ and $D = E = 0$ in equations (53) and (54) are considered, the results align completely with those obtained using a linear method, as described in references [25].

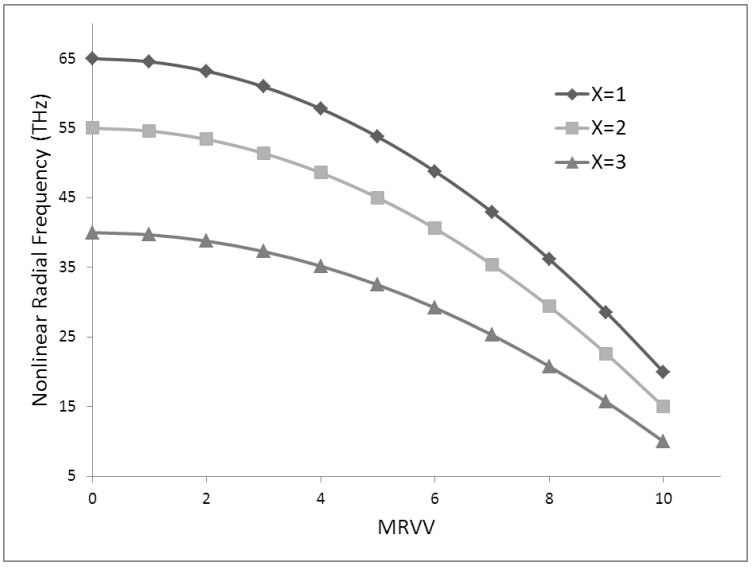

Figure 4. Nonlinear radial natural frequency against nondimensional MRVV for Zigzag (16, 0) and clamped-free boundary condition with different MTVVs

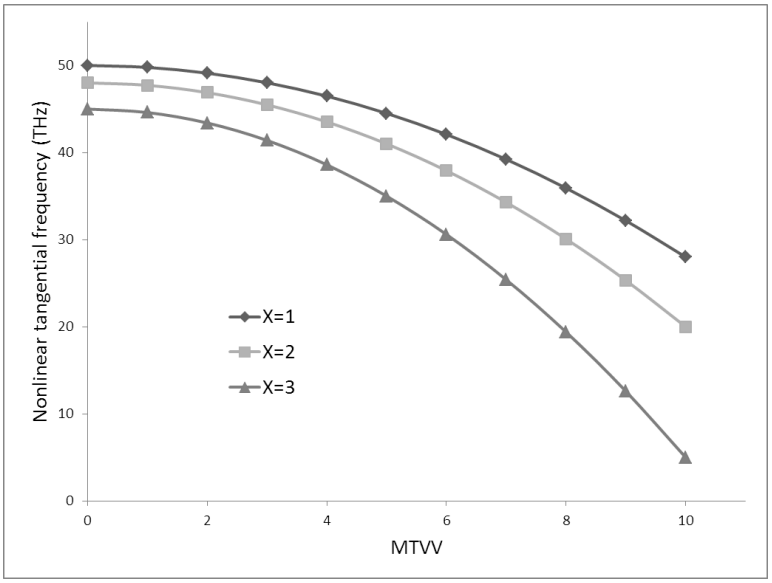

Figure 5. Nonlinear tangential natural frequency against nondimensional MTVV for Zigzag (16, 0) and clamped-free boundary condition with different MRVVs

Figure 6 demonstrates the relationship between nonlinear tangential natural frequency and tube length for a Zigzag (16, 0) single-walled carbon nanotube (SWCNT) under different boundary conditions. The figure shows that as the tube length increases, the nonlinear natural frequencies of the SWCNT decrease, with this reduction being more pronounced at shorter lengths. As anticipated, the clamped nanotube exhibits the highest natural frequency among the boundary conditions examined. Additionally, the data suggest that at greater tube lengths, the nonlinear frequencies tend to converge towards their linear counterparts.

Figure 7 illustrates the variation of nonlinear natural tangential frequency with respect to tube diameter for different vibration modes. As shown, an increase in tube diameter corresponds to an increase in the nonlinear tangential natural frequency. This effect is more noticeable at higher vibration modes and larger tube diameters. The figure also indicates that the nonlinear natural frequency increases with increasing vibration mode.

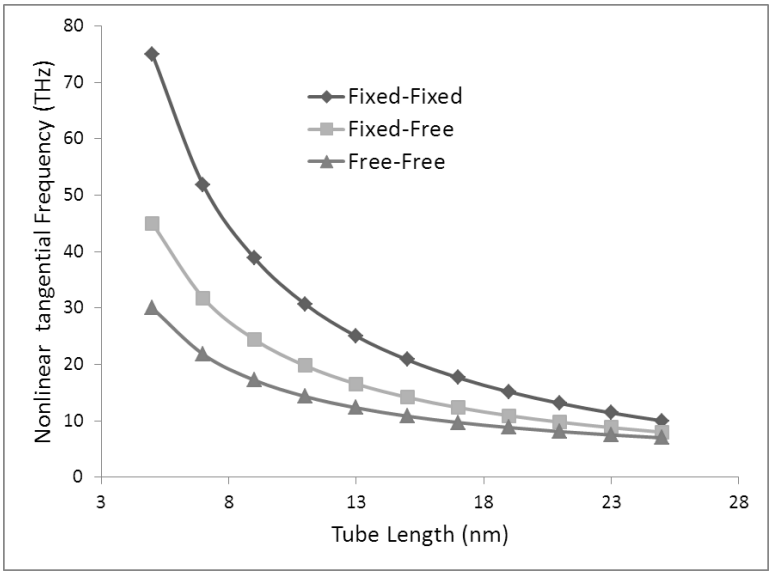

Figure 6. Variation of nonlinear tangential natural frequencies against tube length for Zigzag (16, 0) SWCNT with $X = Y = 1$ under various boundary conditions

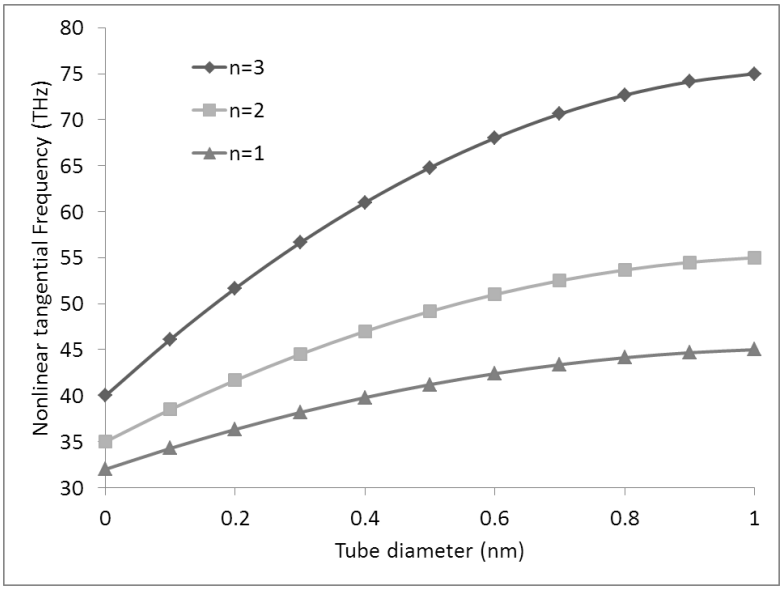

Figure 7. Variation of nonlinear tangential frequency versus tube diameter with $X = Y = 1$ for various vibration modes

Conclusions

This study provides a comprehensive analysis of the nonlinear coupling between tangential and radial vibrations in single-walled carbon nanotubes (SWCNTs) employing the Homotopy Perturbation Method (HPM). The governing equations for this coupled vibration were derived within the framework of new nonlocal continuum mechanics named DM, representing the first application of nonlocal theory to investigate this specific nonlinear interaction in SWCNTs. It is the first time that coupled nonlinear radial-tangential vibration of SWCNTs studied using DM. Also, due to the complexity of the governing equation, the tangential vibration mode has been less studied in scientific researches. The nonlinear behavior originates from large deformations induced by the interaction between radial and tangential vibrational modes. The nonlinear natural frequencies were obtained by applying HPM to the derived nonlinear frequency equations under various boundary conditions. HPM demonstrated itself as a robust and efficient technique for resolving the complex nonlinear partial differential equations governing the coupled tangential-radial vibrations in SWCNTs. The investigation systematically examined the effects of tube radius, tube length, and maximum vibration velocity on the nonlinear natural frequencies across different boundary conditions and mode numbers. The accuracy and reliability of the DM and HPM results were confirmed through excellent agreement with numerical simulations.

Key findings of this research are as follows:

- The coupling between tangential and radial vibrations requires defining nonlinear natural frequencies for both directions. The component of these frequencies independent of vibration velocity corresponds to the natural frequencies of a linear uncoupled model.
- Nonlinear natural frequencies depend on the maximum tangential and radial vibration velocities, reflecting the intrinsic nonlinearity of the system.
- Interaction between radial and tangential vibrations appears in higher-order free vibrations of the SWCNT, arising from large deformation terms within the nonlinear governing equations. This coupling significantly influences the dynamic response of the SWCNT.
- Nonlinearity leads to an increase in natural frequencies relative to linear predictions, with nonlinear frequencies consistently exceeding their linear counterparts.
- Transitioning from clamped-free (C-F) to fully clamped (C-C) boundary conditions results in increased natural frequencies, especially pronounced in shorter tube lengths.
- Increasing tube diameter elevates nonlinear natural frequencies, particularly at higher vibration modes, indicating enhanced nonlinear effects at elevated modes.

Natural frequencies decrease as tube length increases, with this trend more evident under clamped boundary conditions and higher mode numbers,

suggesting a diminishing radial-tangential vibration interaction with longer tubes. Conversely, increasing tube diameter exhibits the opposite effect.

References

[1] Fatahi-Vajari, A. (2018). A new method for evaluating the natural frequency in radial breathing like mode vibration of double-walled carbon nanotubes. *ZAMM. 98*(2), 255-269. https://doi.org/10.1002/zamm.201600234

[2] Ferrari, M., Granik, V. T., Imam, A., & Nadeau, J. (1997). *Advances in Doublet Mechanics*. https://link.springer.com/book/10.1007/978-3-540-49636-6

[3] Bachilo, S., M., Strano, M. S., Kittrell, C., Hauge, R. H., Smalley, R. E., & Weisman, R. B. (2002). Structure-Assigned Optical Spectra of Single-Walled Carbon Nanotubes. *Science*. *298*, 2361-2366. https://doi.org/10.1126/science.1078727

[4] Hussain, M., Alzahrani, A.O.M., Khadimallah, M.A., Alghamdi, S., Fatahi-Vajari, A., & Tounsi, A., (2022). Based on Euler beam theory to evaluate the GHz frequencies versus length-to-radius ratios: Continuum model. Advances in Concrete Construction, 14(4), 291-298. https://doi.org/10.12989/acc.2022.14.4.291

[5] Bandow, S., Asaka, S., Saito, Y., Rao, A., Grigorian, L., Richter, E., & Eklund, P. (1998). Effect of the growth temperature on the diameter distribution and chirality of single-wall carbon nanotubes. *Physics Review Letters. 80*(17), 3779–3782. https://doi.org/10.1103/PhysRevLett.80.3779

[6] Shokri, D., Ebrahimian, M.R., Tabibian, B., Allahverdlou, M.R., Atlasbaf, M.S. (2023). Analytical Response of Nonlinear Buckling of Composite Plates Reinforced with Graphene Nanosheets. *Transactions on Machine Intelligence. 6*(2), 76-88. https://doi.org/10.47176/TMI.2023.76

[7] Gupta S.S., & Batra R.C. (2008). Continuum structures equivalent in normal mode vibrations to single-walled carbon nanotubes. *Computational Materials Science. 43*, 715–723. https://doi.org/10.1016/j.commatsci.2008.01.032

[8] Gupta, S.S., Bosco, F.G., & Batra, R.C. (2010). Wall thickness and elastic moduli of single-walled carbon nanotubes from frequencies of torsional, torsional and in extensional modes of vibration. *Computational Materials Science. 47*, 1049–1059. https://doi.org/10.1016/j.commatsci.2009.12.007

[9] Granik, V.T., Ferrari M., (1993). Microstructural mechanics of granular media. *Mechanics of Materials. 15*, 301–322. https://doi.org/10.1016/0167-6636(93)90005-C

[10] Iijima, S. (1991). Helical microtubes of graphitic carbon. *Nature (London), 354*, 56–58. https://doi.org/10.1038/354056a0

[11] Mahdavinia, M., Ghavidel, A.K., & Kiani, G. (2024). Investigating the Effect of Hard Template Synthesis Method and Diameter Uniformity of Nanocomposite Nanowires based on Polyaniline/Silver Nanoparticles on Electrical and Electrochemical Properties. *Journal of Engineering and Applied Research (JEAR), 1*(1), 55-71. https://doi.org/10.48301/JEAR.2024.191061

[12] Ghosh, P., Soga, T., Afre, R.A., & Jimbo, T. (2008). Simplified synthesis of single-walled carbon nanotubes from a botanical hydrocarbon, Turpentine oil. *Journal of Alloys and Compounds*, *462*, 289–293. https://doi.org/10.1016/j.jallcom.2007.08.027

[13] Mirzamohammadi, S., Hashemi, S. J., & Zal V. (2024). Modification of Nanoparticle Absorption Using Sodium Dodecyl Sulfate Addition in Composite Plating Bath.

Journal of Engineering and Applied Research (JEAR), 1(2), 91-100. https://doi.org/10.48301/JEAR.2024.459185.1028

[14] Movahedi, A., Taghimolaee, M., Ghayebpanah, S., Monajemi, F., Ghanbari , M., & Farhazadi, H. N. (2024). A Review of the Effect of Nanoparticles on Reactive Oxygen Species Production in Different Plants. *Journal of Engineering and Applied Research (JEAR), 1*(1), 131-163. https://doi.org/10.48301/EAR.2024.191062

[15] Mirtalaie, S.H., & Hajabasi, M.A. (2017). Nonlinear axial-lateral-torsional free vibrations analysis of Rayleigh rotating shaft. *Archive of Applied Mechanics, 87*(9), 1465–1494. https:// doi.org/10.1007/s00419-017-1265-6

[16] Ishida, Y., & Yamamoto, T. (2012). *Linear and Nonlinear Rotordynamics*. Wiley-VCH. https://www.wiley.com/en-us/shop/general-energy/linear-and-nonlinear-rotordynamics-a-modern-treatment-with-applications-2nd-edition-p-9783527651917

[17] Fatahi-Vajari, A., & Imam, A. (2016). Lateral vibration of single-layered graphine sheets using doublet mechanics. *Journal of solid mechanics. 8*(4), 875-894. https://oiccpress.com/jsm/article/view/12573

[18] Ansari, R., Gholami, R., Rouhi, H., (2012). Vibration analysis of single-walled carbon nanotubes using different gradient elasticity theories. *Composites: Part B, 43,* 2985–2989. https://doi.org/10.1016/j.compositesb.2012.05.049

[19] Ebrahimian, M.R., Imam, A. & Najafi, M. (2018). Doublet mechanical analysis of bending of Euler-Bernoulli and Timoshenko nanobeams. *ZAMM, 98(* ۹)، 1642-1665. https://doi.org/10.1002/zamm.201700365

[20] Bocko, J., & Lengvarský, P. (2014). Bending Vibrations of Carbon Nanotubes by using Nonlocal Theory. *Procedia Engineering, 96,* 21–27. https://doi.org/10.1016/j.proeng.2014.12.093

[21] Fatahi-Vajari, A., & Imam, A. (2016). Torsional vibration of single-walled carbon nanotubes using doublet mechanics. *ZAMP, 67,* 81.1-81.22 https://doi.org/10.1007/s00033-016-0675-6

[22] Gheshlaghi, B., Hasheminejad, S.M., & Abbasion, S. (2010). Size dependent torsional vibration of nanotubes. *Physica E, 43*, 45– 48. https://doi.org/10.1016/j.physe.2010.06.015

[23] Arda, M., & Aydogdu, M. (2015). Analysis of free torsional vibration in carbon nanotubes embedded in a viscoelastic medium. *Adv. Sci. Technol. Res. J. 9(26),* 28–33. https://doi.org/10.12913/22998624/2361

[24] Ebrahimian, M.R. (2025). Torsion of single-walled carbon nanotubes using new nanomechanical model with considering the chiral effects, *Mechanics of Smart Structures, 1(1),* 1-17. https://doi.org/10.30511/jmms.2025.2061073.1022

[25] Fatahi-Vajari, A., & Imam, A. (2016). Analysis of radial breathing mode of vibration of single-walled carbon nanotubes via doublet mechanics. *ZAMM, 96*(9), 1020–1032. https://doi.org/10.1002/zamm.201500160

[26] Liand, Q.M., & Shi, M.X. (2008). Intermittent transformation between radial breathing and flexural vibration modes in a single-walled carbon nanotube. *Proc. R. Soc. A, 464*, 1941–1953. https://doi.org/10.1098/rspa.2007.0253

[27] Fatahi-Vajari, A., & Imam, A. (2016). Axial vibration of single-walled carbon nanotubes using doublet mechanics. *Indian Journal of Physics, 90*(4), 447–455. https://doi.org/10.1007/s12648-015-0775-8

[28] Demir, C., Civalek, O. (2013). Torsional and longitudinal frequency and wave response of microtubules based on the nonlocal continuum and nonlocal discrete models. *Appllied Mathathematical Modeles, 37*, 9355–9367. https://doi.org/10.1016/j.apm.2013.04.050

[29] Aydogdu, M. (2012). Axial vibration analysis of nanorods (carbon nanotubes) embedded in an elastic medium using nonlocal elasticity. *Mech. Res. Commun, 43,* 34–40. https://doi.org/10.1016/j.mechrescom.2012.02.001

[30] He, J.H. (1998). Approximate analytical solution for seepage flow with fractional derivatives in porous media. *Computer Methods in Applied Mechanics and Engineering, 167*, 57-68. https://doi.org/10.1016/S0045-7825(98)00108-X

[31] He, J.H. (2006). Homotopy perturbation method for solving boundary value problems. *Physics Letters, Section A. 350*(1-2), 87–88. https://doi.org/10.1016/j.physleta.2005.10.005 [32] Vahidi, A.R., Azimzadeh, Z., & Didgar, M. (2013). An efficient method for solving Riccati equation using homotopy perturbation method. Indian Journal of Physics, 87(5), 447-454. https://doi.org/10.1007/s12648-012-0234-8

[33] Azimzadeh, Z., Vahidi, A.R., & Babolian, E. (2012). Exact solutions for non-linear Duffing's equations by He's homotopy perturbation method. Indian Journal of Physics, 86(8), 721-726. https://doi.org/10.1007/s12648-012-0115-1

[34] Cveticanin, L. (2009). Application of homotopy-perturbation to nonlinear partial differential equations. *Chaos, Solitons & Fractals, 40(1),* 221–228. https://doi.org/10.1016/j.chaos.2007.07.053

[35] Ebrahimian, M.R., Imam, A. & Najafi, M. (2020). The effect of chirality on the torsion of nanotubes embedded in an elastic medium using doublet mechanics. *Indian Journal of Physics*, 94, 31–45. https://doi.org/10.1007/s12648-019-01455-1

[36] Basirjafari, S., EsmaeilzadehKhadem, S. & Malekfar, R. (2013). Radial breathing mode frequencies of carbon nanotubes for determination of their diameters, *Current Applied Physics, 13(3)*, 599-609. https://doi.org/10.1016/j.cap.2012.11.001